44th Aerospace Sciences Meeting and Exhibit
January 9-12, 2006 Reno, NV
AIAA-2006-0260

Considerations for Aerodynamic Testing of Scaled Runback Ice Accretions

Edward A. Whalen*, Andy P. Broeren† and Michael B. Bragg‡
University of Illinois at Urbana-Champaign, Urbana, IL, 61801

Runback ice accretions present a unique problem in iced-airfoil aerodynamics in that the airfoil typically has a clean leading edge prior to the ice shape itself. In order to investigate the aerodynamic effects of runback ice accretions simulated ice shapes were scaled, from accretions obtained in testing at the NASA Glenn Icing Research Tunnel, for testing in the UIUC 3'x4' subsonic wind tunnel. Simple geometric scaling, based on airfoil chord, as well as boundary-layer scaling, based on estimated boundary-layer thickness, was used. The NACA 3415 and the NACA 23102 were tested at a Reynolds number of $1.8x10^6$ and Mach number of 0.18 with and without the simulated ice shapes attached. Simple 2-D simulations were constructed for the test as well as 3-D simulations that used multiple substrate layers as well as roughness to simulate the features of the full-scale accretion. Significant penalties due to runback accretions were identified. The NACA 3415 experienced a 20% reduction in C_{lmax} and no loss in stalling angle of attack due to the 3-D warm hold simulation while the NACA 23012 experienced a 25% reduction in C_{lmax} and a loss of two degrees in stalling angle of attack. The 3-D cold hold simulation caused a 40% loss in C_{lmax} and a two degree reduction in stalling angle of attack for the NACA 3415 while the same ice shape caused a 55% reduction in C_{lmax} and a seven degree reduction in stalling angle of attack for the NACA 23012. Geometrically-scaled 2-D simulations of the warm hold accretions were found to enhance the lift performance of the NACA 3415 and had little effect on the NACA 23012. The cause of this phenomenon is hypothesized to be a combination of energizing the boundary-layer and the pressure distribution established by the presence of the ridge shape. The boundary-layer-scaled equivalent of that ice shape was observed to reverse this phenomenon. Boundary-layer calculations indicated that the geometrically-scaled ice shape was approximately the same height as the local boundary thickness at angles of attack near stall. The boundary-layer-scaled ice shapes were observed to cause greater penalties than both the 2-D and 3-D geometrically-scaled ice shapes. Boundary-layer-scaled 3-D ice shapes remain to be tested. It should be noted that data regarding the effect of full-scale runback ice accretions are not available at this time. Therefore, it is difficult to judge which scaling method is appropriate. However, it is clear from this work that geometric scaling may not be sufficient for scaling runback-type ice accretions for aerodynamic testing.

Nomenclature

α	= angle of attack
$\alpha_{l,0}$	= zero-lift angle of attack
α_{stall}	= stalling angle of attack
c	= model chord length
C_d	= drag coefficient
$C_{d,0}$	= zero-lift drag coefficient
C_l	= lift coefficient
C_{lmax}	= maximum lift coefficient
C_m	= quarter-chord pitching moment coefficient
C_p	= pressure coefficient
k	= ice height or thickness
M	= Mach number

* Graduate Research Assistant, Department of Aerospace Engineering, Member AIAA.
† Research Scientist, Department of Aerospace Engineering, Senior Member AIAA.
‡ Professor and Head, Department of Aerospace Engineering, Fellow AIAA.

Re = Reynolds number
U = local airspeed
U_∞ = freestream airspeed
x = chordwise position along airfoil

I. Introduction

Runback ice accretions occur on thermal anti-icing systems when the system is not evaporating 100% of the water impinging in the surface. In that case the water runs back to the point where the added heat no longer raises the surface temperature above freezing. The water begins to freeze, developing a ridge line and leaving the leading edge clean. In the case of hot air systems, extensive spanwise variation is possible due to the arrangement of the jets that provide the surface heating.

Runback icing is a potential problem in some phases of flight for example, holding in icing and descent through icing conditions. Holding greatly increases the exposure time and can challenge the system during high water catch rates or very low temperatures. The descent phase is also critical because the engine power is reduced and therefore less mass flow and lower temperature air is being provided to the system.

As with all icing studies, aerodynamic penalties are of particular concern. Studies by Jacobs,[1] Lee et al.[2] and others have clearly demonstrated the impact of ice shapes on aerodynamic performance. Lee, in particular, studied ridge shapes, although not necessarily runback ridges, and found dramatic loses in lift and increases in drag. Jacobs placed a k/c=0.005 spoiler at various chordwise positions on a five-inch chord NACA 0012 at $Re=3.1x10^6$. His study was mostly concerned with the drag effects of manufacturing protuberances. He observed much more substantial reductions in C_{lmax} for the same shape attached at x/c=5% (almost 50%) versus those attached at x/c=15% (less than 15%). Calay et al.[3] simulated runback ridges using a step, a ramp and a triangular shape, each with k/c=0.0035, on a NACA 0012 at $Re=1.25x10^6$ and found that drag increased up to 30% while C_{lmax} decreased up to 20%. He also found that the same shapes at x/c=15% increased the C_{lmax} of the airfoil. The greatest C_{lmax} increase was approximately 5% and α_{stall} was delayed by one degree. Calay noted that the stall of the airfoil with the simulated ice shapes began from the ice shape rather than from the trailing edge, as is the case for the clean airfoil. He attributed the increase in C_{lmax} to the ice shape causing the flow to remain attached at greater angles of attack than in the clean case. Calay concluded that small changes in the ice configuration were able produce large changes in the performance effect requiring accurate simulations to estimate actual runback effects. Papadakis and Gile-Laflin[4] also observed increases in airfoil performance due to a backward facing ramp with k/c=0.0041 at x/c=15% and a spoiler with k/c=0.0053 at x/c=15%. Their tests were conducted using a modified NACA 63_A213 airfoil at $Re=2.0x10^6$. The ramp increased C_{lmax} by 9% and delayed stall by four degrees. The spoiler increased C_{lmax} by 1% and delayed stall by one degree. Tests with the ramp at x/c=2.5% resulted in an 18% loss in C_{lmax} and a two degree reduction in stalling angle of attack.

Testing the aerodynamic performance penalties of runback ice accretions is one aspect of the hot-air anti-icing systems research at the University of Illinois (UIUC). Ice accretion testing at the Icing Research Tunnel (IRT) at NASA Glenn utilized a model that was not suitable for generating castings for aerodynamic performance testing. Therefore, the ice accretions were geometrically-scaled from the full scale model to the model size used in the UIUC 3'x4' subsonic wind tunnel. The results of both the icing and aerodynamic tests were published in 2005 by Whalen et al.[5] A phenomenon was later observed in which α_{stall} and C_{lmax} increased with the addition of certain runback ice shapes. Since these tests were conducted at below full-scale Reynolds number and at x/c locations where the boundary layer is thicker, ice-shape scaling was a concern. To address these topics the calculated boundary-layer thickness was used to scale the runback ice shapes. This paper reviews the testing of simulated warm and cold hold runback ice shapes scaled both geometrically and based on local boundary-layer thickness. The mechanism for increasing the stalling angle of attack and maximum lift coefficient is also discussed.

II. Experimental Methods

Aerodynamic tests of simulated runback ice accretions were conducted in the UIUC 3'x4' subsonic wind tunnel. The models tested had a chord of 18 inches and spanned the entire height of the test section. Two models, the NACA 23012 and the NACA 3415, were selected to provide a range of clean airfoil characteristics. The NACA 23012 model had 68 chordwise pressure taps and 19 spanwise pressure taps. The NACA 3415 model had a trailing edge flap that was set at zero degrees deflection for this test. The model had 78 chordwise pressure taps and 13 spanwise pressure taps.

Fig. 1 Experimental setup in the UIUC 3' x 4' wind tunnel.

A three-component force balance was used to measure the lift and pitching moment and the integrated turntable was used to set the angle of attack. The force balance was located below the test section and supported the model. Figure 1 is a photograph of the experimental setup. The model and traverse-mounted wake rake are shown in the photograph. The wake rake had 59 total pressure probes that were used to acquire the wake pressures. Both the wake and airfoil surface pressures were acquired with an electronically scanned pressure system. More information about the setup can be found in Lee.[6] Simple 2-D shapes as well as 3-D simulated runback accretions, scaled with respect to chord length, were tested on both the NACA 3415 and the NACA 23012. The ice shapes tested were representative of the specific conditions tested in the IRT. The simulations were made using measurements taken from that test and by reproducing the features observed on the castings of the full scale accretions. The results contained in this report correspond to the runback ice shapes observed at the chosen conditions for warm hold, cold hold, etc. In general, the conditions were chosen to represent the worst case for each of the icing conditions, as described in section I.

Although surface pressure distributions were available, the lift coefficient and quarter-chord pitching-moment coefficient were derived only from the force-balance. The pressure and balance data agreed very well for the clean model configuration. However, larger differences were observed for the iced-model configurations because surface pressures could not be resolved accurately in the vicinity of simulated ice accretions. In addition, the runback ice shapes often covered a large chordwise area, eliminating multiple pressure taps and causing the integrated force and moment to be incorrect. Therefore, the data the balance were more accurate. The drag coefficient was calculated from the wake pressures using standard momentum-deficit methods. All of these aerodynamic coefficients and the angle of attack were corrected for wall interference effects using the methods of Rae and Pope.[7] The experimental uncertainty in these coefficients was also estimated using the methods of Kline and McClintock[8] and Coleman and Steele[9] for 20:1 odds (Table 1). The uncertainties in α, C_l and C_m were determined from the force-balance data and the remaining quantities (C_p, C_d) were determined from the pressure-based data. The values were determined by Lee[6] and Lee and Bragg[10] for freestream conditions of Re = 1.8×10^6 and M = 0.18. All data reported in this paper correspond to this freestream condition.

Table 1 Estimated experimental uncertainties.

Aerodynamic Quantity	Reference Value	Absolute Uncertainty	Relative Uncertainty
α	5.00	±0.02	±0.40%
C_p	-0.712	±0.0037	±0.52%
C_l	0.295	±0.0016	±0.53%
C_m	-0.0791	±0.00039	±0.50%
C_d	0.0102	±0.00014	±1.40%

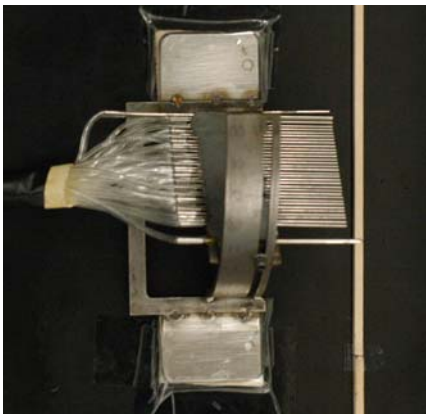

Fig. 2 Boundary-layer "rake" shown (viewed from above) attached to model.

In addition to aerodynamic performance measurements, two other tools were used to evaluate the effect of the ice accretions on the airfoils. Boundary-layer profile measurements were taken using a boundary-layer "rake" (Fig. 2). The "rake" used the local static pressure obtained from the nearest airfoil pressure tap with total pressures measured using an

array of pitot tubes to calculate the local airspeed. Fluorescent oil flow visualization was also used to identify specific flow features and aid in the interpretation of airfoil surface pressure data.

III. Results and Discussion

A. Geometrically-scaled versus Boundary-layer-scaled Ice Shapes

Aerodynamic performance testing of geometrically-scaled runback ice shapes was conducted in 2004. The ice shapes were scaled based upon the ratio of the mid-span chord of the IRT model to the chord of the UIUC models. The mid-span chord of the IRT model is 61" and the chord of the UIUC models is 18", making the scaling factor 0.295. Aerodynamic performance testing of boundary-layer-scaled runback ice accretions was completed in May 2005. Boundary-layer scaling was thought to be appropriate since the height of the full scale ice shapes was on the order of the local boundary-layer thickness. The ice shapes were scaled based upon the conditions at which they were originally accreted in the IRT. Namely, the Reynolds number, Mach number and angle of attack were used as inputs to a boundary-layer code that calculated the boundary-layer thickness at the ice accretion locations. The code used integral boundary-layer parameters obtained from XFOIL[11] with the Falkner-Skan[12] solution for a laminar boundary layer and the Coles wake[13] solution for a turbulent boundary layer. Boundary-layer scaling was used to approximate the effect these ice shapes would have on airfoil performance at higher, full-scale, Reynolds numbers. The model used to collect the ice accretions did not yield ice castings that were practical for full-scale testing and a full-scale facility was not readily available for this research effort. Table 2 and Table 3 compare the heights of the ice shapes scaled geometrically and using the boundary-layer height. Scaling was carried out at $\alpha=3^o$, the angle of attack at which the ice was accreted. The boundary-layer thickness is a function of angle of attack, causing k/δ to decrease as angle of attack is increased. The boundary-layer-scaled ice shapes were over twice as tall as the geometrically-scaled ice shapes for the same case. Differences in boundary-layer growth on the two airfoils are more apparent in the warm hold case because the ice shapes occur farther aft on the airfoil.

Table 2 Warm Hold Ice Shape Scaling (x/c=16%, upper surface)

	Geometric Scaling			Boundary-layer Scaling		
Airfoil	k (in.)	k/c	k/δ	k (in.)	k/c	k/δ
Full Scale	0.232	0.0038	5.35	0.232	0.0038	5.35
NACA 23012	0.068	0.0038	2.44	0.149	0.0083	5.35
NACA 3415	0.068	0.0038	3.11	0.117	0.0065	5.35

Table 3 Cold Hold Ice Shape Scaling (x/c=2.8%, upper surface)

	Geometric Scaling			Boundary-layer Scaling		
Airfoil	k (in.)	k/c	k/δ	k (in.)	k/c	k/δ
Full Scale	0.412	0.0068	28.4	0.412	0.0068	28.4
NACA 23012	0.122	0.0068	12.5	0.278	0.0154	28.4
NACA 3415	0.122	0.0068	12.6	0.276	0.0153	28.4

Figure 3 compares the effects on the performance of the NACA 3415 of a geometrically-scaled 3-D warm hold ice shape to that of the 2-D ice shape. For this study, both the upper and lower-surface accretions were simulated. In the 3-D case an effort was made to simulate the finer spanwise features of the ice shapes using simple shapes such as wood strips and roughness. On the suction surface, the height of the initial ridge, 0.0625", was similar to the 2-D case however the chordwise extent of the overall ice shape was much greater, approximately 1.5 inches, compared to that of the 2-D ice shape, which was 0.0625" in chordwise extent. On the lower surface the 3-D simulation had a height between 0.15 and 0.25" that included roughness and a chordwise extent of 0.3" while the 2-D ice shape had a height of 0.21" and a chordwise extent of 0.25". The lower surface ice shape was placed at x/c=19.6%. Details including the dimensions and construction of all the geometrically-scaled ice shapes can be found in Whalen et al.[5] The 3-D ice shape was observed not to have a significant effect on α_{stall}, but did reduce C_{lmax} by over 20%. A 2-D simulation based on the maximum height measured from the full scale accretion is also included. The ice shape had a height of 0.094" (k/c=0.0052). However, it was not representative of the overall ice shape because it was based on an isolated feature of the accretion. It does demonstrate though, that there was a significant change in the effect of the ice shape at this location at heights between 0.0625", where there was a lift performance increase, and 0.094",

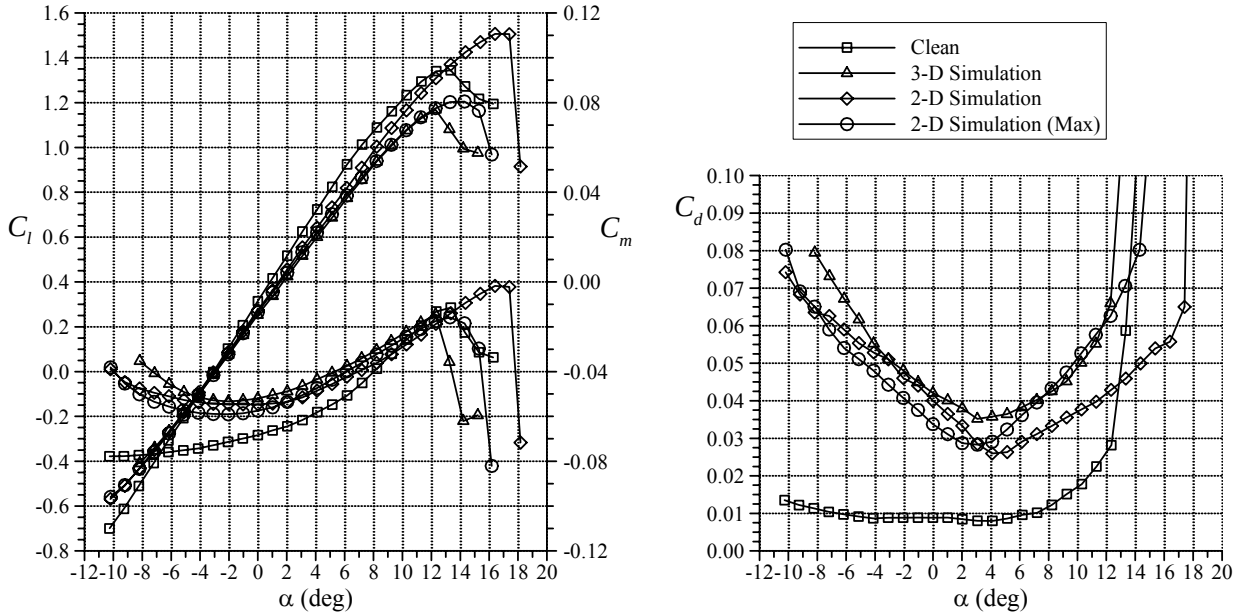

Fig. 3 Comparison of the effect of simulated 3-D and 2-D geometrically-scaled warm hold ice shapes on the lift, drag and pitching moment of the NACA 3415 (Re=1.8x10^6, M=0.18).

where there was a lift performance penalty. Figure 4 presents the performance effects of the same ice shape simulations on the NACA 23012. In contrast to the NACA 3415, the NACA 23012 exhibits an abrupt stall, indicating that it naturally stalls from the leading-edge. McCullough and Gault[14] conducted extensive investigations into airfoil stall and found that leading edge stall is typical of airfoils of moderate thickness like the NACA 23012,

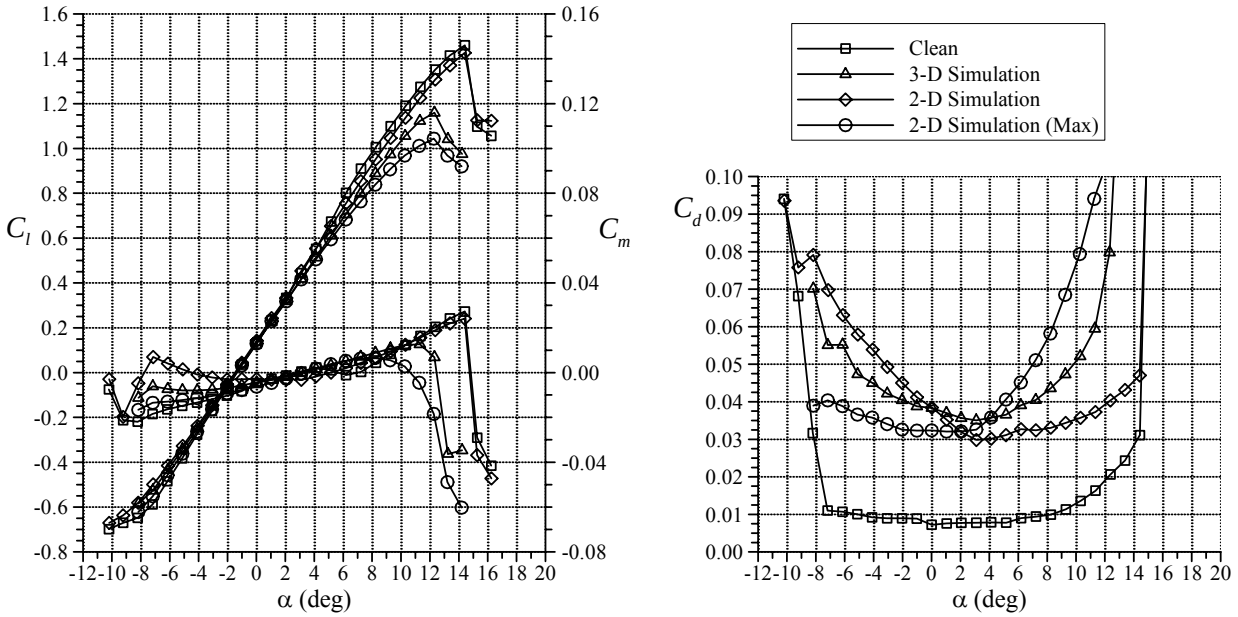

Fig. 4 Comparison of the effect of simulated 3-D and 2-D geometrically-scaled warm hold ice shapes on the lift, drag and pitching moment of the NACA 23102 (Re=1.8x10^6, M=0.18).

while trailing edge stall is typical for thicker airfoils like the NACA 3415. The geometrically-scaled 2-D ice shape had little effect on the lift performance of the NACA 23012. However, for the drag was increased to a similar degree to that of the NACA 3415. The 2-D simulation based on the maximum measured height again had a substantial effect on the performance, similar to that of the 3-D simulation, and appeared to alter the stalling character of the airfoil. The lower-surface ice shape for that case was not based on the maximum height of the

lower-surface ice shape, and was actually slightly shorter, with a height of 0.17", than the actual 2-D simulation, so that the drag at low and negative C_l was lower than in the 2-D simulation. This was also observed on the NACA 3415, but to a lesser degree. The 3-D simulation caused a 25% decrease in C_{lmax} and a two degree reduction in stalling angle of attack. It also caused a change in the stalling behavior of the airfoil. It is important to note that in all these cases the presence of the simulation reduces the lift curve slope, it is only at high angle of attack that the geometrically-scaled 2-D ice shape is able to achieve any improvement in performance.

The performance penalties of geometrically-scaled 2-D and 3-D cold hold ice shapes on the NACA 3415 are compared in Fig. 5. The upper surface 3-D ice shape had a height between 0.094" and 0.125" and a chordwise extent of approximately 0.6". The lower surface 3-D ice shape had a height of 0.1" and a chordwise extent of 0.6".

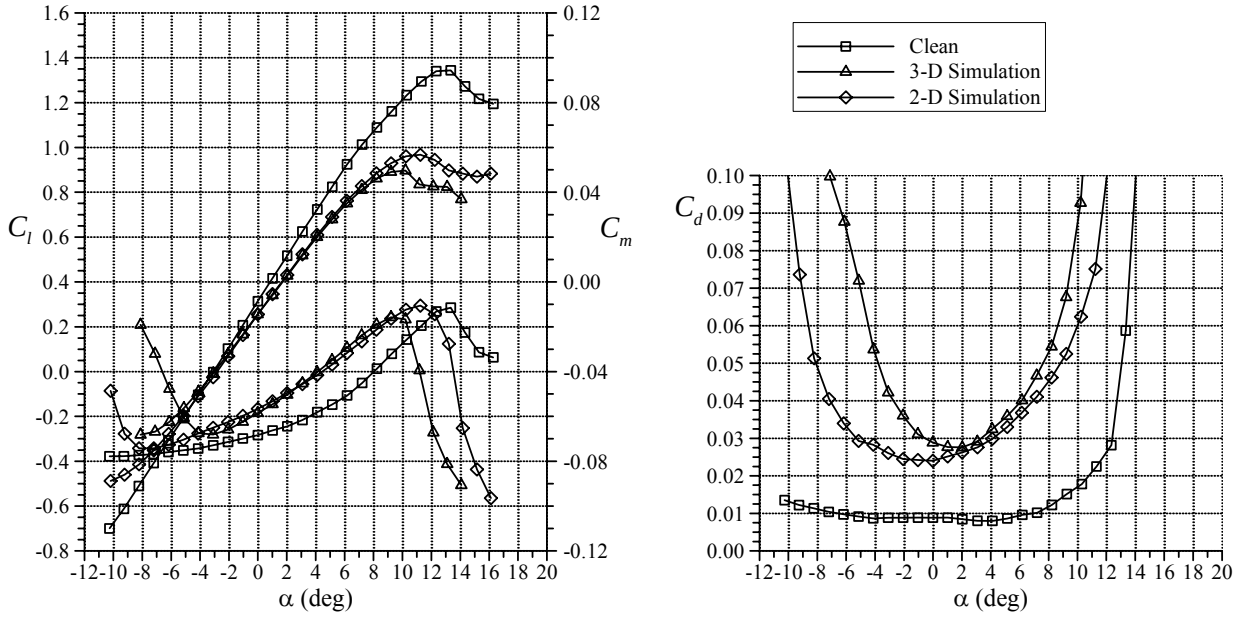

Fig. 5 Comparison of the effect of simulated 2-D and 3-D geometrically-scaled cold hold ice shapes on the lift, drag and pitching moment of the NACA 3415 (Re=1.8x10^6, M=0.18).

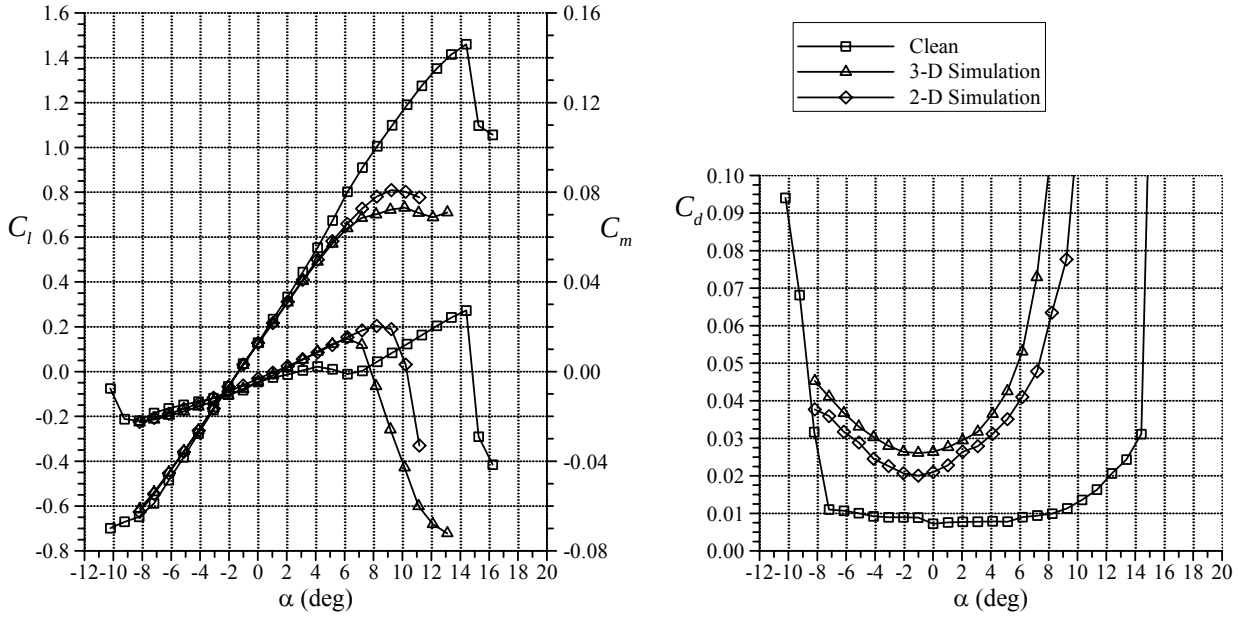

Fig. 6 Comparison of the effect of geometrically-scaled simulated cold hold ice shapes on the lift, drag and pitching moment of the NACA 23102 (Re=1.8x10^6, M=0.18).

The 2-D ice shape had a height of 0.125" and chordwise extent of 0.125" on the upper surface and a height of 0.094" and chordwise extent of 0.094" on the lower surface. The upper surface shape was attached at x/c=1.5% and the lower surface shape was attached at x/c=3.5%. The 3-D ice shape reduced the maximum lift coefficient by 40%, 10% more than the 2-D simulation, and caused a loss of three degrees in stalling angle of attack compared to a loss of two degrees in the 2-D case. Drag results were quite similar at moderate to high angles of attack and actually less than those observed for the warm hold case. The lower-surface ridge in the warm hold case was quite large compared to the cold hold case, which was evident in the warm hold drag polar at low and negative angles of attack. In addition the upper-surface accretion, though shorter in height, was over twice as long in chordwise extent. Performance penalties experienced by the NACA 23012 due to geometrically-scaled 2-D and 3-D ice shapes are presented in Fig. 6. The 2-D ice shape caused a 45% reduction in C_{lmax} and a loss of five degrees in stalling angle of attack. The 3-D ice shape caused a similar performance penalty to that caused by the 2-D ice shape. The loss in C_{lmax} was approximately 10% greater than the 2-D case and there was an additional three degree loss in stalling angle of attack. In this case, these numbers are based on the break in the pitching moment defining α_{stall} since the C_l does continue to rise past that point. In general, the cold hold ice shapes had a greater effect on the NACA 23012 because of the higher pressure peak and steeper recovery that develops near the leading edge when compared to the NACA 3415. Also, the cold hold ice shapes were, in general, more detrimental to the performance of the airfoils than were the warm hold ice shapes.

Figure 7 presents the effect of simulated 2-D warm hold ice shapes on the performance of the NACA 3415. The upper-surface ice shapes alone are presented to demonstrate the difference between the boundary-layer and

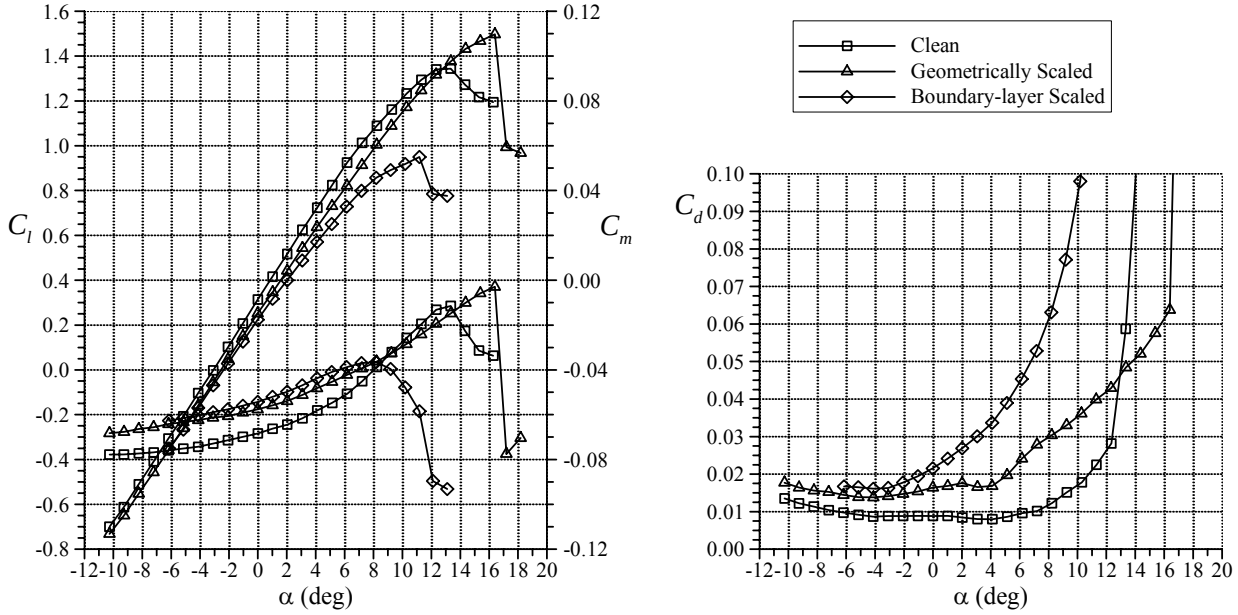

Fig. 7 Effect of a simulated 2-D warm hold ice shape (upper-surface only) on the lift, drag and pitching moment of the NACA 3415 ($Re=1.8x10^6$, M=0.18).

geometrically-scaled ice shape. The simulated geometrically-scaled ice shape refers to an ice shape created by taking an average height and chordwise location, taken from ice measurements as well as castings, and scaling that height based upon the ratio of the chord of the sub-scale model to that of the full scale model (i.e. matched k/c). The boundary-layer-scaled ice shape refers to the same ice shape scaled by the ratio of the local boundary-layer thickness of the sub-scale model to the full scale model (i.e. matched k/δ). The goal of the 2-D ice shapes was to simulate the initial ridge rather than the entire extent of the ice shape. In the geometrically-scaled case, a 0.0625" (k/c=0.0035) square section of balsa was positioned at x/c=16% to simulate the warm hold ice shape. Interestingly, α_{stall} increased by four degrees and the C_{lmax} increased by over 10%. This is the effect that motivated the investigation of Reynolds number as a factor in the performance effects of these ice shapes. Note that the character of the stall changed as a result of the geometrically-scaled ice shape. It became much more abrupt in both the loss of lift and the change in the pitching moment. The boundary-layer-scaled ice shape was a 0.125" square section of balsa also

positioned at x/c=16% and caused a 30% decrease in C_{lmax} and a two degree reduction in stalling angle of attack. For the boundary-layer ice shape, the stall character appeared to be more like that of the clean airfoil.

Performance effects on the NACA 3415 of simulated 2-D cold hold ice shapes on the upper surface only are presented in Fig. 8. The upper-surface ice shapes alone are presented to demonstrate the difference between the boundary-layer and geometrically-scaled ice shape. The 2-D geometrically-scaled ice shape was simulated using a 0.125" (k/c=0.007) section of balsa at x/c=2.8%. The 2-D boundary-layer-scaled ice shape was simulated using a 0.25" (k/c=0.014) section of balsa at x/c=2.8%. The geometrically-scaled ice shape caused a 30% loss in C_{lmax} and a one degree decrease in stalling angle of attack. The boundary-layer-scaled ice shape resulted in a nearly 50% loss in C_{lmax} and a five degree reduction in stalling angle of attack. The increase in drag was similarly more substantial for the boundary-layer-scaled ice shape. These results are contrasted with the warm hold results for the NACA 3415 where the geometrically-scaled ice shape actually improved the performance. In this case, both the geometrically-scaled ice shape and the boundary-layer-scaled ice shape are over four times taller than the local boundary-layer height. This suggests that the proper scaling method may be a function of the ice-shape location and size. Therefore, scaling cold hold ice shapes geometrically, similar to unprotected ice shapes or other ice shapes with leading-edge contamination, may be appropriate because of their height relative to the boundary layer. In fact, leading-edge ice shapes are typically scaled geometrically and have exhibited good agreement with full-scale tests of castings and 2-D simulations.[15,16]

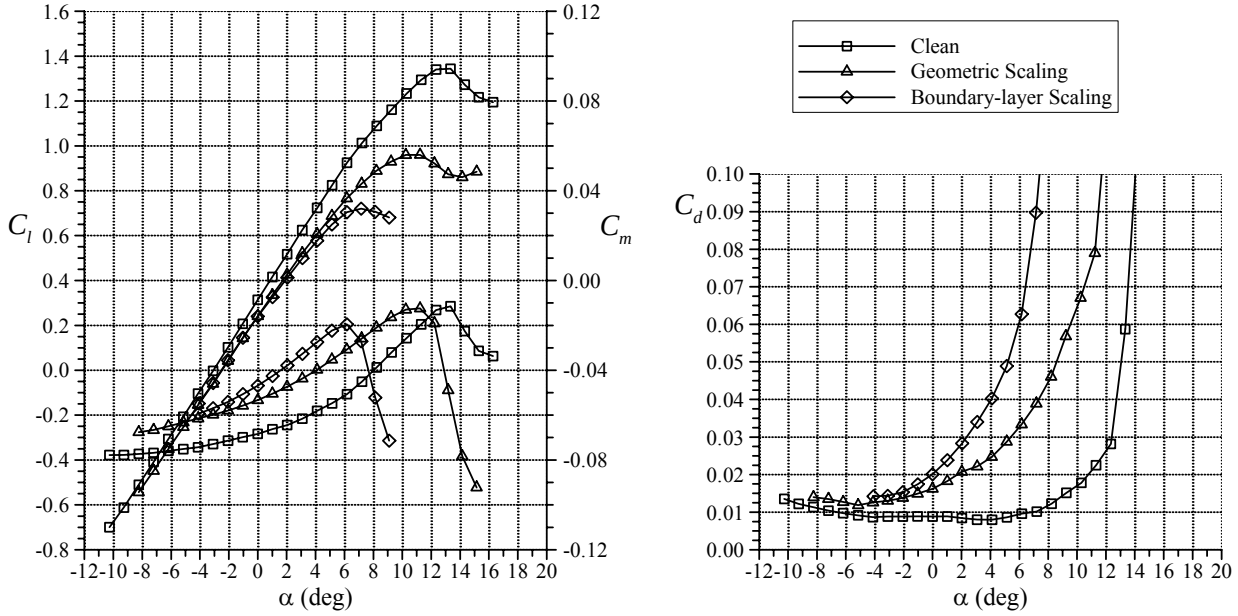

Fig. 8 Effect of simulated 2-D cold hold ice accretion on the lift, drag and pitching moment of the NACA 3415 (Re=1.8x10^6, M=0.18).

An investigation into the effect of the chordwise extent of the 2-D ice accretion simulations was conducted after observing some of the differences between the 2-D and 3-D simulations. Figure 9 presents the effect, on the NACA 23012, of chordwise extent of the ice accretion simulations for 0.0625" tall (k/c=0.0035) ice shapes at x/c=10%. Although the chordwise extent does have some effect at x/c=5%, for both pitching moment and lift coefficient it appears to reach some limit with increasing chordwise extent. Interestingly, the lift performance penalty decreased with increasing cordwise extent. At x/c=10%, the penalty of the 0.0625" ice shape is first made less by increasing the chordwise extent then increases again when the extent is 0.5". The effect of chordwise extent for 0.125" tall (k/c=0.007) ice shapes at x/c=5% and x/c=10% was small and acted to reduced the penalty of the ice shape with the smallest chordwise extent (0.0625"). At 10% there was again an increase in the penalty when the chordwise extent was 0.5", but it did not become greater than the 0.0625" extent ice shape. This result was similar to that observed for the 0.0625" tall ice shape. Figure 10 presents the effect of chordwise extent of the ridges at x/c=5% and x/c=10% for both a 0.0625" and 0.125" tall ice shape on the zero-lift angle of attack and zero-lift drag. The clean value of both of these parameters is included in the plots as a bold line. It can be seen that the 0.0625" ice shape causes $\alpha_{l,0}$ to become less negative as the chordwise extent is increased (Fig. 10 (a)), in effect de-cambering the airfoil. The 0.125" ice shape appears to have a similar effect, but it is less significant than in the 0.0625" tall shape

case. Chordwise extent acted to reduce the zero-lift drag increase caused by the both the 0.0625" and 0.125" tall shapes (Fig. 10 (b)).

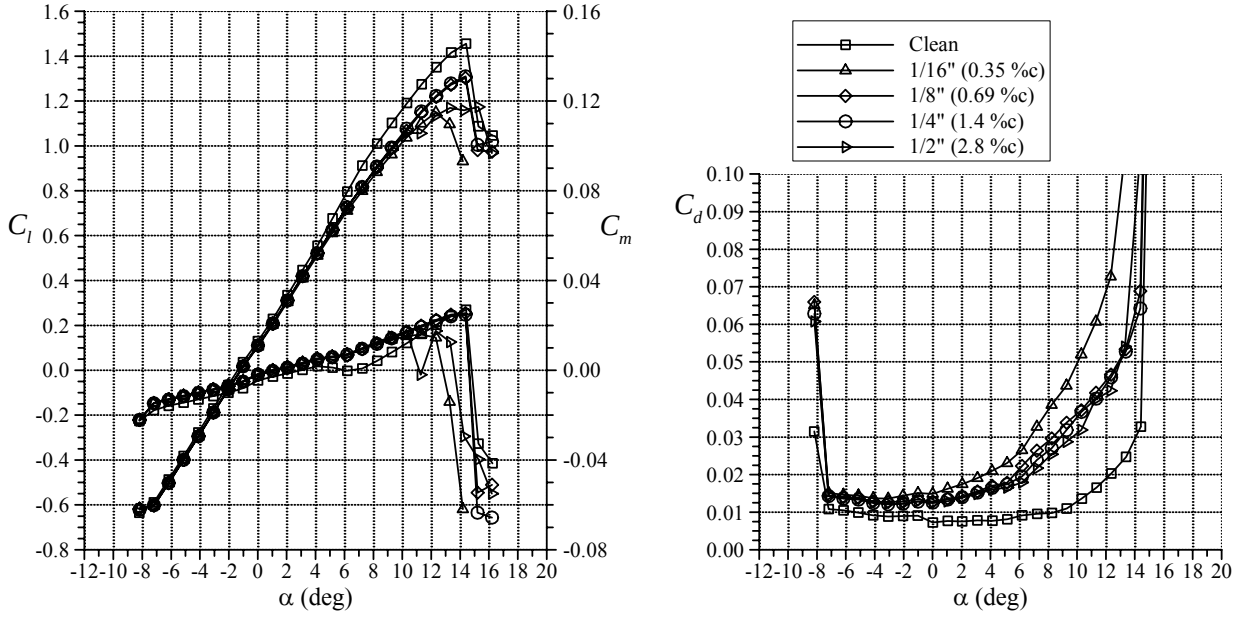

Fig. 9 Effect of chordwise extent of a 0.0625" tall (k/c=0.0035) simulated runback ice shape at x/c=10% on the lift, drag and pitching moment of the NACA 23102 (Re=1.8x10^6, M=0.18).

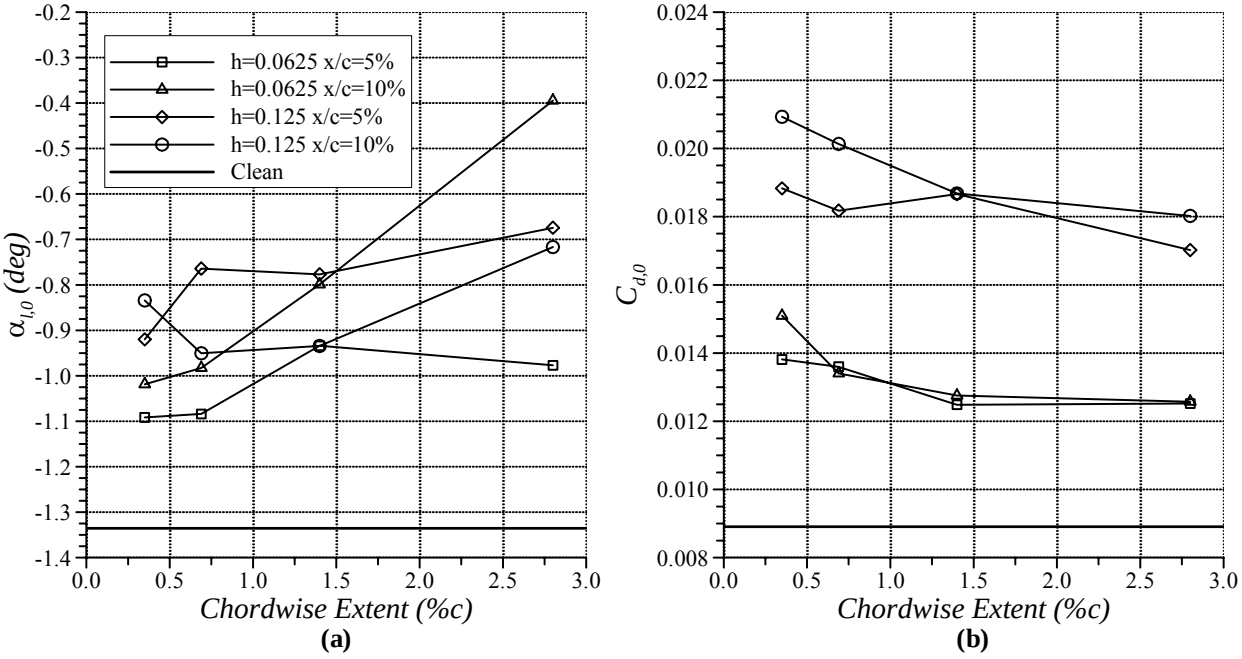

Fig. 10 Effect of chordwise extent of 0.0625" and 0.125" tall ridges at x/c=5% and 10% on the $\alpha_{l,0}$ and $C_{d,0}$ of the NACA 23012 (Re=1.8x10^6, M=0.18).

B. Lift Enhancement due to Ridge-type Ice Shapes

Another motivation for exploring the boundary-layer scaling of these ice shapes was to investigate the phenomenon by which α_{stall} and C_{lmax} are increased by the presence of the geometrically-scaled warm hold ice shapes. Results from florescent oil flow visualization for the NACA 3415 at $\alpha=16^o$ with the 0.0625" ice shape located at x/c=16% are presented in Fig. 11. Sixteen degrees angle of attack corresponded to C_{lmax} for this case (Fig. 7). Transition was apparent near the leading edge, followed by a faint zone at approximately x/c=22% where the flow reattached after separating from the ice shape. Trailing-edge separation then occurred between x/c=60% and x/c=65%. Stall in this case resulted from the collapse of the leading-edge pressure peak that was developed because of the separation bubble just aft of the ice shape. In the case of the boundary-layer-scaled ice shape, which had a height of 0.125", the reattachment zone moved aft rapidly with angle of attack. Figure 12 shows the florescent oil flow visualization results for the NACA 3415 with the boundary-layer-scaled 2-D warm hold ice shape. The corresponding performance data were presented in Fig. 7. In Fig. 12 (a), corresponding to $\alpha=6^o$, the reattachment zone following separation from the ice shape was clearly visible near x/c=35%. At $\alpha=8^o$ (Fig. 12 (b)) trailing-edge separation

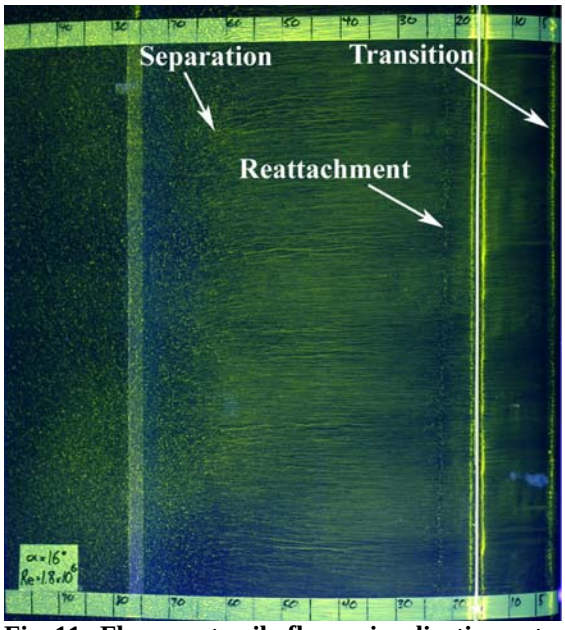

Fig. 11 Florescent oil flow visualization at $\alpha=16^o$ for the NACA 3415 with the geometrically-scaled 2-D warm hold shape attached. ($Re=1.8x10^6$, M=0.18)

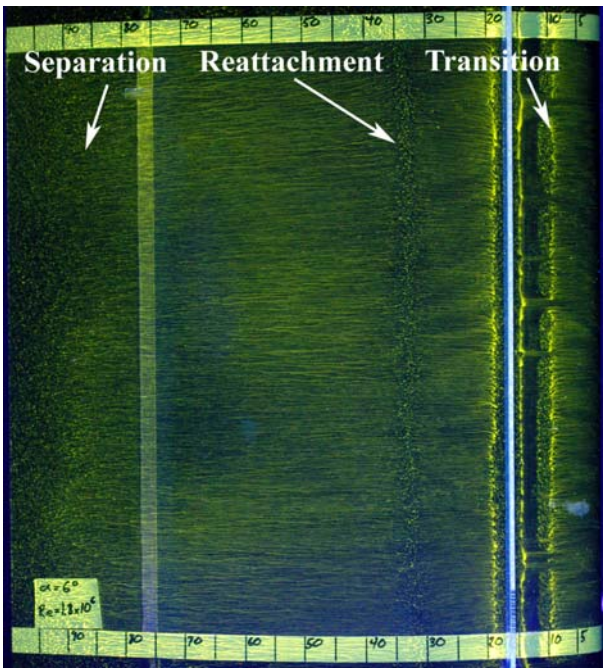

(a) $\alpha=6^o$

(b) $\alpha=8^o$

Fig. 12 Florescent oil flow visualization at $\alpha=6^o$ (a) and $\alpha=8^o$ (b) for the NACA 3415 with the boundary-layer-scaled 2-D warm hold ice shape attached. ($Re=1.8x10^6$, M=0.18).

moved forward slightly and reattachment moved aft by approximately 5%. At $\alpha=9^o$, there appeared to be some reverse flow where the separation bubble was, however there was not attached flow following the line that divided the reverse flow from the flow aft of it. This indicated that the bubble was no longer closed and the flow was separating from the ice shape and not reattaching to the airfoil. In the case of the 0.125" ice shape, separation progressed forward rapidly from the trailing edge to meet the separation bubble growing rearward to cause stall.

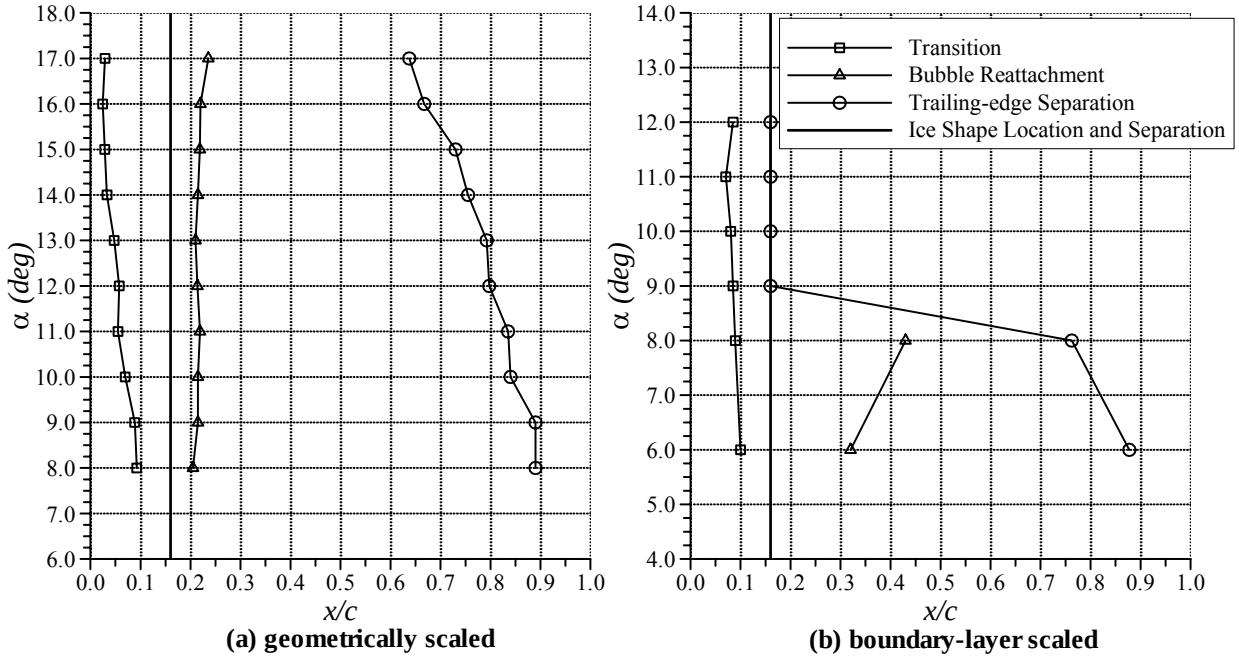

(a) geometrically scaled **(b) boundary-layer scaled**

Fig. 13 Florescent-oil flow visualization analysis with (a) the geometrically-scaled and (b) the boundary-layer-scaled warm hold ice shape at x/c=16% (NACA 3415, Re=1.8x10^6, M=0.18).

The results of the flow visualization are summarized in Fig. 13. Flow visualization showed that trailing-edge separation progressed rapidly forward as angle of attack increased and that the separation bubble was much larger than in the geometrically-scaled case. The separation bubble in the geometrically-scaled case remained approximately 5 to 7% of the chord up to stall (Fig. 13 (a)) and trailing-edge separation progressed only to approximately x/c=65% at stall. In the boundary-layer-scaled case, the separation bubble was 30 to 40% of the chord (Fig. 13 (b)). In addition, the flow appeared to be separated directly from the ice shape at angles of attack greater than eight degrees. Figure 14 illustrates the effect of ice shape height at x/c=16% on the performance of the NACA 3415. Two ice shape heights, in addition to the actual 2-D geometrically-scaled warm hold ice shape, were also tested. Stall was delayed by the 0.0625" (k/c=0.0035), as discussed earlier, and 0.08" (k/c=0.0044) ice shapes. However, the 0.094" (k/c=0.005) ice shape reduced the C_{lmax} of the airfoil and maintained the same α_{stall} as the clean airfoil. Recall that the geometrically-scaled ice shape had a k/c=0.0035 and the boundary-layer-scaled ice shape had a k/c=0.007.

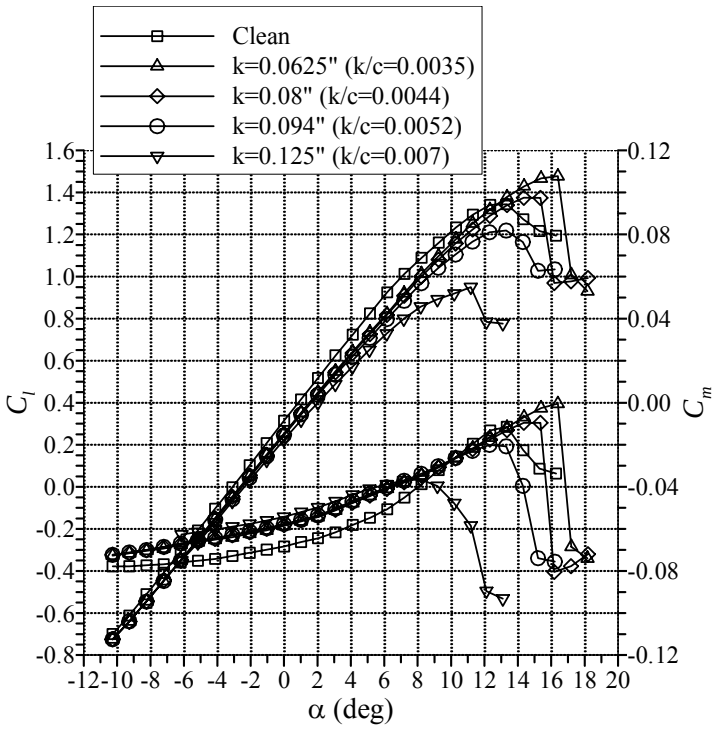

Fig. 14 Effect of ice shape height at x/c=16% on the NACA 3415 (Re=1.8x10^6, M=0.18)

Figure 15 compares the k/δ values as a function of C_l/C_{lmax} for the ice shapes tested in the present study to those tested by Calay[3] and Papadakis[4]. In each case, the boundary-layer height was calculated for the clean airfoil.

The Reynolds number for these cases ranged from $1.25x10^6$ to $2.0x10^6$. The Calay and Papadakis shapes were located at x/c=15% versus x/c=16% for the present study. Ice shapes that were observed to cause a performance increase had a k/δ near one as the airfoil approached C_{lmax}. In contrast to those ice shapes, the boundary-layer scaled ice shape, with a height of 0.125", had a k/δ greater than two up to stall. This demonstrated that the relative height of the ice shape to the boundary layer plays a significant role in the phenomenon. It also showed that simple geometric scaling of runback ice accretions may not be sufficient to accurately describe their aerodynamic effects. Figure 16 shows boundary-layer profile measurements for the geometrically-scaled 2-D ice shape at $\alpha=10^o$. Figure 17 shows boundary-layer profile measurements for the boundary-layer-scaled 2-D ice shape. The boundary-layer flow is quite different between the two ice shapes. Pitot tubes were used to collect the pressure probe data from which airspeed was calculated. Because pitot tubes do not read correctly in areas of reverse flow these areas are indicated as zero airspeed in the figures. In the case of the geometrically-scaled ice shape, the only zero airspeed reported was at the lowest pitot tube positioned at approximately 0.01" from the model surface. At heights of 0.03 and

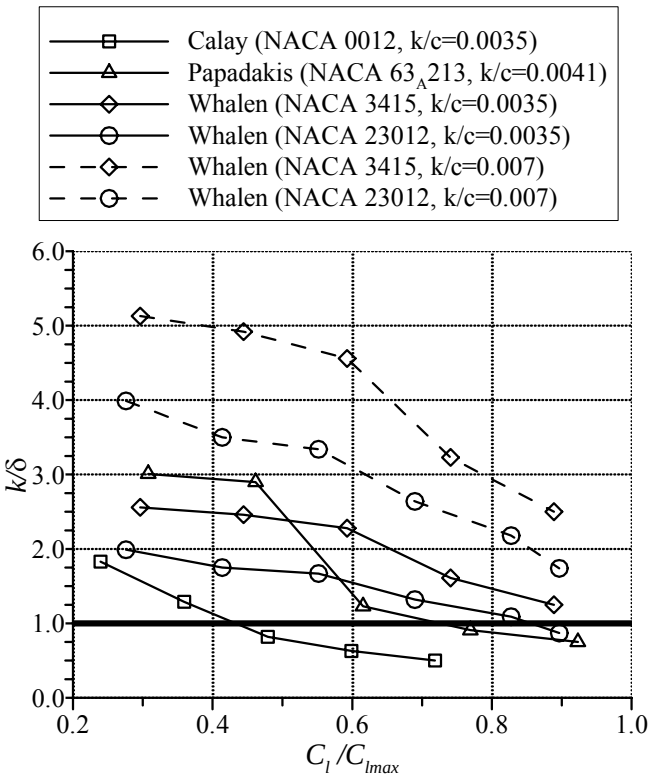

Fig. 15 Comparison of k/δ for various ice shapes at x/c=15% (Calay[3] and Papadakis[4]) and 16% (Whalen).

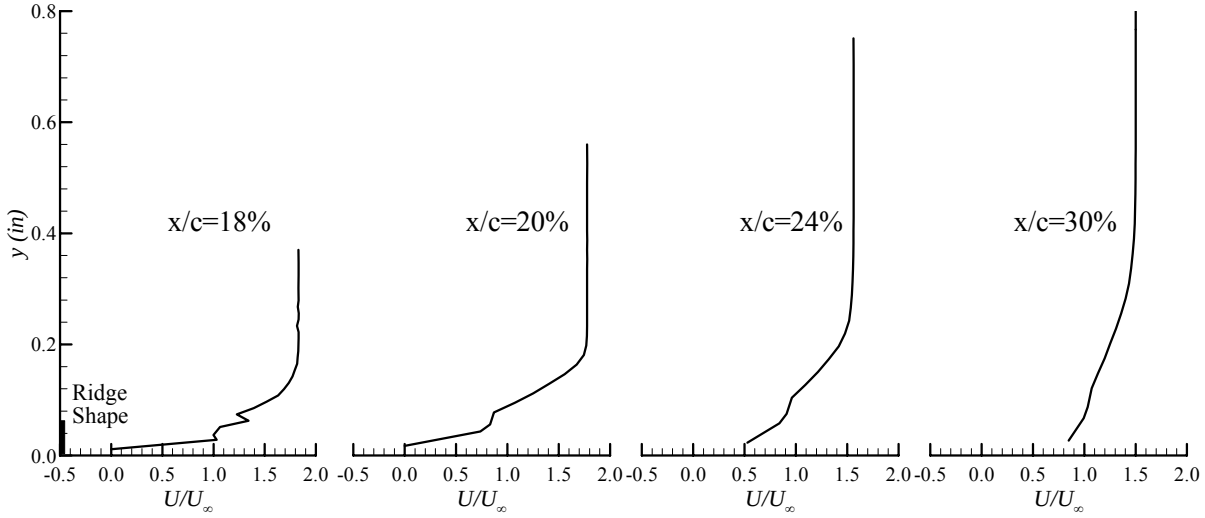

Fig. 16 Boundary-layer profile measurements at $\alpha=10^o$ for the geometrically-scaled 2-D warm hold ice shape at x/c=18%, 20%, 24% and 30% (NACA 3415, $Re=1.8x10^6$, M=0.18).

0.06 there were sharp increases in the local airspeed. Subsequent measurements at x/c=20%, 24% and 30% showed that these features were not present by x/c=20%. However, some remnant of these features persisted, manifested as a slope change in the profile that remains within the boundary-layer, to x/c=30%, the farthest aft station where measurements were taken. At x/c=20% the slope change extends from approximately 0.04" to 0.08" and at x/c=30% the slope change extends from approximately 0.06" to 0.12". The increased edge velocity was also echoed in the pressure profiles at these angles of attack (Fig. 18). In the pressure profiles the local edge velocity, derived from surface pressure measurements, was greater than that on the clean model up to approximately x/c=25%. The

boundary-layer profiles for the boundary-layer-scaled ice shape showed a large region of reverse flow that reached a maximum height of 0.2" near x/c=24% and decreased in height by x/c=30%. Flow visualization showed that the separation bubble reattached near x/c=42%. Clearly, the geometrically-scaled ice shape is able to modify the boundary-layer flow while only creating a small, stable, separation bubble while the boundary-layer-scaled ice shape generates a large separation bubble. This modification apparently allows the boundary-layer to remain attached at angles of attack greater than the clean stalling angle of attack by energizing it and delaying the advancement of the trailing-edge separation. The large separation bubble generated by the boundary-layer-scaled ice shape removes momentum from the boundary layer and hastens the advancement of the trailing-edge separation, causing the airfoil to stall earlier.

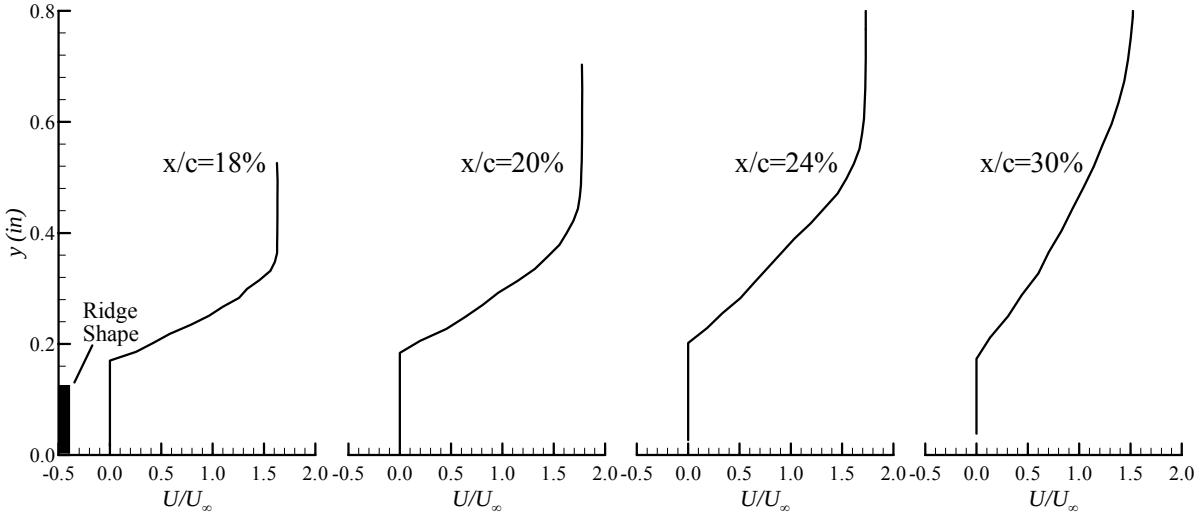

Fig. 17 Boundary-layer profiles measurements at $\alpha=8^o$ for the boundary-layer-scaled 2-D warm hold ice shape at x/c=18%, 20%, 24% and 30% (NACA 3415, Re=1.8x10^6, M=0.18).

Analysis of the pressure distributions on the model as a result of these ice shapes indicated another effect besides energizing the boundary-layer, which both Calay[3] and Papadakis[4] point to as the cause of the lift benefit. Figure 18 (a) shows the pressure profiles for the NACA 3415 with the 0.0625" runback ice simulation installed at x/c=16%. The first thing to note is the sharp increase in the magnitude of C_p following the ice shape. In addition, the suction peak at the leading edge was allowed to grow to over 30% greater than the clean suction peak. The ability of the airfoil to sustain the higher suction peak and the added low pressure in the vicinity of the ice shape generated lift coefficients that were larger than in the clean case. It is important to note that up to $\alpha=13^o$ the pressure peak was lower in magnitude, for the same angle of attack, with the ice shape installed than it was in the clean case. The less negative C_p preceding the ice shape, as compared to the clean C_p in the same location, was caused by stagnation of the flow in front of the ice shape. In addition, the flow accelerated over the ice shape, generating an abrupt increase in the magnitude C_p. The subsequent rapid decrease in the magnitude of C_p and return to the clean C_p indicated the presence of a short separation bubble following the ice shape. This caused a reduction in the lift curve slope at low angle of attack. At angles of attack greater than the clean stalling angle of attack the delay in trailing-edge separation caused by the ice shape allowed the circulation of the airfoil to continue to increase, driving the stagnation point farther aft on the lower surface and resulting in greater flow acceleration near the leading edge. The recovery that followed the second pressure peak was gentle in comparison to that of the leading-edge peak and, in fact, was comparable to the recovery at thirteen degrees, and decreased in slope with angle of attack. Ultimately the gradients developed by the leading-edge peak were too great and the suction peak collapsed as the boundary-layer separated from the ridge and failed to reattach. Oil flow visualization showed that after stall the flow was still attached up to the ridge. In the case of the 0.125" ice shape (Fig. 18 (b)) the pressure preceding the ice shape is much grater than seen with the 0.0625" ice shape, approximately -0.4 versus -1.8. Trailing-edge separation appeared to be extensive; this was confirmed by flow visualization (Fig. 12). The airfoil was unable to generate a substantial leading-edge suction peak due to the separation and stagnation ahead of the ice shape. In fact, the secondary peak, caused by flow acceleration around the ice shape, was greater in magnitude than the leading-

edge suction peak. In addition, the low pressure region caused by the ice shape was greater in chordwise extent, indicating the greater extent of the separation bubble in that case. The secondary peak accounted for the fact that the lift was not substantially more penalized at low angles of attack when compared to the effect of the 0.0625" ice shape (Fig. 7). Pressure profiles with ice shapes of intermediate heights were also collected. The pressure peak was slightly reduced in magnitude by the 0.08" tall ice shape, compared to the 0.0625" tall case, and the local acceleration area was wider and had a more gentle recovery. The sudden and almost entire separation of the flow from the airfoil again occurred. In the case of the 0.094" tall ice shape, the local low pressure in the vicinity of the ice shape was less than that caused by the previous two ice shapes, reaching a minimum C_p of approximately -2.5 versus -3.0 for the shorter ice shapes. In addition, the pressure preceding the ice shape was greater. That is, the stagnation region achieved a C_p of -1.0 while the previous ice shapes resulted in a C_p of -1.8 and -1.5 for the 0.0625" and 0.08" ice shapes, respectively. The pressure peak near the leading edge was less than in the clean case, which accounts for the decreased maximum lift coefficient (Fig. 14). The reduction in the pressure peak was caused by the extraction of momentum by the separation bubble which led to greater trailing-edge separation, effectively de-cambering the airfoil. This effect further reduced C_{lmax} as the ice-shape height was increased. Recall that the lift performance effect changed drastically between the 0.08" and 0.094" ice shapes (Fig. 14). The 0.094" ice shape caused a performance penalty by enhancing the natural trailing-edge stall of the NACA 3415 rather than preventing it. The change in stalling behavior was confirmed by flow visualization for the 0.125" ice shape (Figs. 12 and 13 (b)), which had a similar post-stall pressure distribution to the 0.094" tall ice shape.

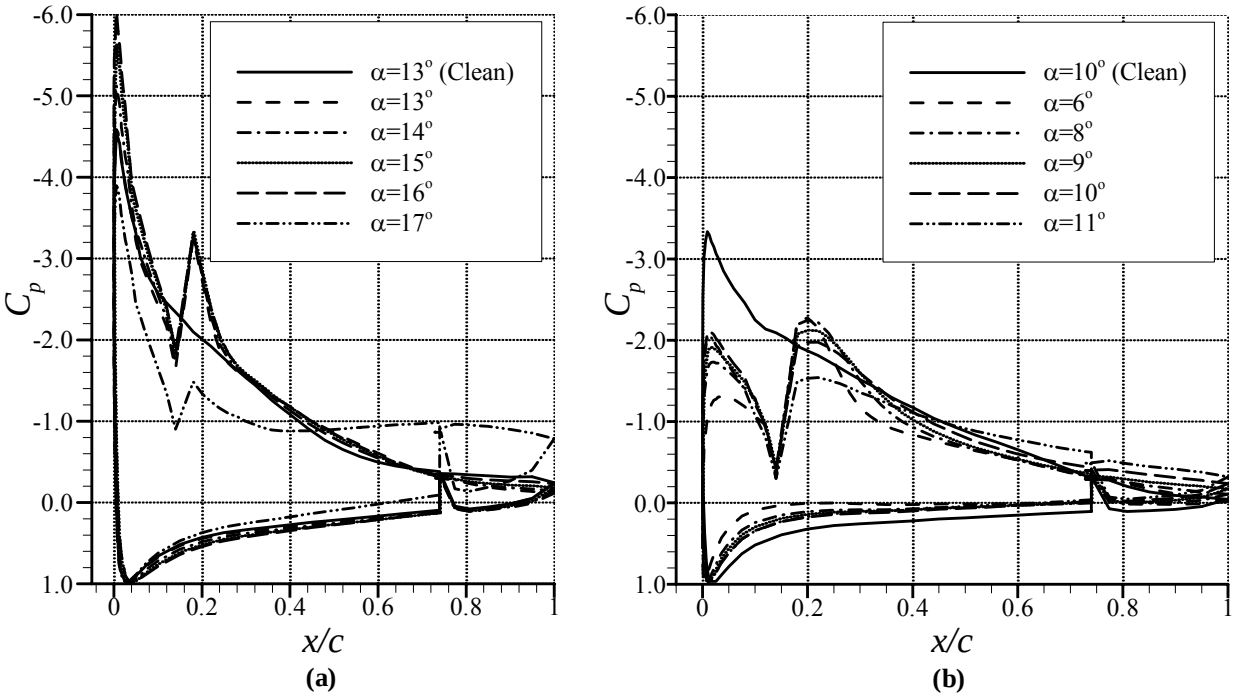

Fig. 18 NACA 3415 pressure profiles near stall with 0.0625" (a) and 0.125" (b) ice shape installed at x/c=16% (Re=1.8x10^6, M=0.18).

IV. Conclusions

The effects of runback ice accretions on the NACA 3415 and NACA 23102 were explored using simulated ice shapes scaled for testing in the UIUC 3'x4' wind tunnel. Geometrically-scaled three-dimensional simulations of both cold and warm hold runback ice shapes were tested. The warm hold ice shapes were found to reduce the C_{lmax} of the NACA 3415 by 20% and did not affect the stalling angle of attack. The same ice shapes reduced the C_{lmax} of the NACA 23012 by 25% and caused a two degree reduction in stalling angle of attack. The cold hold ice shapes reduced the C_{lmax} of the NACA 3415 by 40% and led to a two degree reduction in stalling angle of attack, while the NACA 23012 experienced a 55% reduction in C_{lmax} and a loss of seven degrees in stalling angle of attack. Drag results showed that in general the warm hold ice shapes caused a greater penalty than the cold hold ice shapes. Although the upper-surface cold hold ice shape was taller than the warm hold ice shape, the warm hold ice shape

had over twice the chordwise extent. In addition, the lower-surface warm hold ice shape was taller than the cold ice shape.

Two scaling methods were used in this study. The first method was a simple geometric scaling according to the chord length of the full scale and UIUC models. In previous studies, this method has been shown to accurately scale ridge accretions near the leading edge.[15,16] It was found that the geometrically-scaled warm hold ice shapes, which were located at x/c=16%, were on the order of the boundary-layer thickness in height or shorter at high angle of attack when scaled in this manner. The second method utilized the boundary-layer thickness to scale the ice shapes. The boundary-layer scaling method was employed to attempt to take into account the effect of Reynolds number on these ice shapes. The boundary-layer-scaled ice shapes were over twice as tall as the corresponding geometrically-scaled ice shapes and consequently led to greater penalties, especially in the lift performance. It is important to recognize that runback ice accretions present a unique problem with regard to aerodynamic testing. The fact that the airfoil is clean leading up to the ice shapes, the ridges are relatively short and that, in the warm hold case, the ridges are quite far aft results in Reynolds number considerations and effects potentially being important to characterizing the aerodynamic penalties of these ice shapes.

Tests with two-dimensional simulations resulted in a variety of performance effects. Shorter upper-surface ridges were able to modify the stalling behavior of the NACA 3415, which exhibits a trailing-edge-type stall naturally. The same ice shapes had little effect on the performance of the NACA 23012. Boundary-layer-scaled ice shapes led to greater performance penalties than both the 2-D and 3-D geometrically-scaled ice shapes. The boundary-layer scaled warm hold ice shape generated a large separation bubble that grew rapidly with angle of attack and removed momentum from the boundary layer, accelerating the progression of the trailing-edge stall. Additional testing of boundary-layer-scaled 3-D ice shapes on both of these airfoils remains to be conducted.

The maximum lift and stalling angle of attack was observed to increase due to the geometrically-scaled warm hold ice shape. Two phenomena were identified that contributed to this phenomenon. First, the generation of a small separation bubble acted to energize the boundary-layer and caused the trailing-edge separation to progress forward more slowly. Because the flow remained attached, up to x/c=65% at stall, the circulation of the airfoil increased resulting in a strong leading edge suction peak. Ultimately, the airfoil stalled when the flow separated from the ice shape resulting in an abrupt loss of lift. Second, a low pressure region and secondary pressure recovery set-up by the ridge allowed the leading edge suction peak to grow past the clean peak.

There are currently no data on the aerodynamic effects of runback ice simulations on airfoils at full scale Reynolds number. Therefore, there is little to which these results can be compared. Research to generate these ice shapes and test them at full scale Reynolds number is ongoing within our group at UIUC.

Acknowledgements

The authors would like to recognize several people who made this research program possible. The authors at the University of Illinois were supported, in part, by the FAA under grant DTFA 96-G-023. We would also like to thank Dr. Jim Riley and Mr. Gene Hill, from the FAA. We would like to acknowledge the Icing Branch at NASA Glenn for supporting the ice accretion testing. Specifically, we would like to thank Mr. Gene Addy, Mr. Tom Bond, Dr. Sam Lee and the staff at the IRT.

References

[1] Jacobs, E.N., "Airfoil Characteristics as Affected by Protuberances," NACA Report 446, 1932.

[2] Lee, S. and Bragg, M.B., "Experimental Investigation of Simulated Large-Droplet Ice Shapes on Airfoil Aerodynamics," *Journal of Aircraft*, Vol. 36, No. 5, Sept.-Oct., 1999.

[3] Calay, R.K., Holdo, A.E., Mayman, P., "Experimental Simulation of Runback Ice," *Journal of Aircraft*, Vol. 34, No. 2, Mar.-Apr., 1997.

[4] Papadakis, M., Gile-Laflin, B.E., "Aerodynamic Performance of a Tail Section with Simulated Ice Shapes and Roughness," AIAA 2001-0539, Reno, NV, January, 2001.

[5] Whalen, E.A., Broeren, A.P., Bragg, M.B. and Lee, S., "Characteristics of Runback Ice Accretions on Airfoils and their Aerodynamic Effects," AIAA 2005-1065, Reno, NV, January, 2005.

[6] Lee, S., "Effect of Supercooled Large Droplet Icing on Airfoil Aerodynamics," Ph.D. Dissertation, Dept. of Aeronautical and Astronautical Eng., Univ. of Illinois, Urbana, IL, 2001.

[7] Rae, W.H., and Pope, A., *Low-Speed Wind Tunnel Testing*, Wiley, New York, 1984, pp. 349-362.

[8] Kline, S.J., and McClintock, F.A., "Describing Uncertainties in Single-Sample Experiments," *Mechanical Engineering*, Vol. 75, Jan. 1953, pp. 3-8.

[9] Coleman, H.W., and Steele, W.G., *Experimentation and Uncertainty Analysis for Engineers*, John Wiley and Sons, New York, 1989, pp. 40-118.
[10] Lee, S., and Bragg, M.B., "Experimental Investigation of Simulated Large-Droplet Ice Shapes on Airfoil Aerodynamics," *Journal of Aircraft*, Vol. 36, No. 5, Sept.-Oct. 1999, pp. 844-850.
[11] Drela, M., XFOIL Subsonic Airfoil Development System, *http://raphael.mit.edu/xfoil/*.
[12] White, F.M., *Viscous Fluid Flow*, 2nd Edition, McGraw-Hill, 1991, pp. 242-247.
[13] Coles, D., "The Law of the Wake in the Turbulent Boundary-layer," *J. Fluid Mechanics*, Vol. 1, pp. 191-226, 1956.
[14] McCullough, G.B. and Gault, D.E., "Examples of Three Representative Types of Airfoil-Section Stall at Low-Speed," NACA TN-2502, September, 1951.
[15] Broeren, A.P. and Bragg, M.B., "Effect of Airfoil Geometry on Performance with Simulated Intercycle Ice Accretions," *Journal of Aircraft*, Vol. 42, No. 1, Jan.-Feb., 2005, pp.121-130.
[16] Broeren, A.P., Lee, S., LaMarre, C.M. and Bragg, M.B., "Effect of Airfoil Geometry on Performance with Simulated Ice Accretions Volume 1: Experimental Investigation," FAA Report DOT/FAA/AR-03/64, Aug. 2003.